

Experimental and Numerical Simulation of the Effect of Particles on Flow Structures in Secondary Sedimentation Tanks

H. Asgharzadeh, B. Firoozabadi[†] and H. Afshin

School of Mechanical Engineering, Sharif university of Technology, Tehran, Iran

[†]Corresponding Author Email: firoozabadi@sharif.edu

(Received February 19, 2010; accepted October 24, 2010)

ABSTRACT

Sedimentation tanks are designed for removal of floating solids in water flowing through the water treatment plants. These tanks are one of the most important parts of water treatment plants and their performance directly affects the functionality of these systems. Flow pattern has an important role in the design and performance improvement of sedimentation tanks. In this work, an experimental study of particle-laden flow in a rectangular sedimentation tank has been performed. Kaolin was used as solid particles in these experiments. Also, a numerical simulation was developed using the finite volume method with a k-ε turbulent model. The results of the numerical model agree well with the experimental data. Hydrodynamic parameters and flow patterns of the fresh water flow and particle-laden flow are also compared in this study. The results show that the existence of particles completely changes the flow structures. It seems that the main reason for this phenomenon is the particles settling. Our experimental observations and numerical results show that parameters such as the maximum streamwise velocity, fully developed location, shear stress coefficient at the bottom of the tank and so on are different in water-containing particles compared to pure water and the inlet concentration strongly intensifies the differences.

Keywords: Experimental investigation, Numerical simulation, k-ε turbulent model, Rectangular sedimentation tank, Particle-laden flows.

NOMENCLATURE

C	concentration	σ_k	turbulent prandtl number
C_0	inlet concentration	σ_c	schmidt number
C_d	shear stress coefficient at the bottom of tank	ρ	density
D_p	particle diameter	ρ_w	water density
g	Gravitational acceleration	ρ_p	particle density
g'	reduced gravitational acceleration	v_s	falling velocity
G_b	production term by buoyancy	μ	fluid viscosity
G_k	production term for turbulent kinetic energy	μ_t	turbulent flow viscosity
p	pressure	ν_t	turbulent kinematic viscosity
u, v	Cartesian coordinate velocity	\mathcal{G}	Fluid kinematic viscosity
U_0	inlet velocity	k	turbulent kinetic energy
W	Wind speed	ε	turbulent dissipation energy
z	Height from the bed	τ_w	shear stress at the bottom of tank
$Z_{u \max}$	height of maximum velocity	Z_{neg}	height of negative velocity

1. INTRODUCTION

Solids removal is probably the main process in water purification method in filtration plants. The most significant phase of this process is the separation of sludge and suspended particles from water by means of gravity. In these basins, the turbid water flows into the basin at one end and the cleaner water is taken out at the other end by decanting. Obviously, the water must flow in the tank long enough for appropriate particles deposition. The performance of these sedimentation tanks directly affects the filtration basin's efficiency.

Sedimentation tanks are divided into two main categories. The primary settling tanks have a low influent concentration and the flow field in them is not influenced much by concentration field due to the negligible buoyancy effects. The secondary or final-settling tanks have a higher influent concentration and they are usually placed after the primary and activation tanks (Tamayol *et al.* 2008). So they usually contain activated sludge and hence, the size of particles would grow and flow field is influenced by concentration distribution. Generally, the sedimentation tanks are characterized by several hydrodynamic phenomena, such as density waterfalls, bottom current and surface return currents, and are also sensitive to temperature fluctuations and wind effects.

Various studies have been conducted to find the effects of particles on the flow and hydraulics of settling tanks.

Imam and McCorquodale (1983) solved flow equations with a constant turbulent eddy diffusivity assumption. Celik and Rodi (1985) and Stamou and Rodi (1990) used k- ϵ turbulence model to predict the flow field in settling tanks. Kerbs (1995) developed one and two dimensional models for clarifier modeling. He observed that worse sludge quality causes stronger density current and thus increases the tendency for short circuiting between the inlet and the outlet. Zhou *et al.* (1997) applied a 3-dimensional fully mass conservative clarifier model, based on modern computational fluid dynamics theory. They observed that the upward buoyant flow occurs in the tank with deep sludge blanket and a short circuiting flow appears near the water surface and flow regime is strongly affected by the sludge blanket in the tank. Mazzolani *et al.* (1998) developed numerical models for the prediction of turbulent flow and suspended solid distribution in the sedimentation tank. They found that increasing the concentration in region between discrete settling and hindered settling, results in an increase in settling velocities of the faster particles. In addition, the application of the three distinct settling models in the numerical analysis of the transport in a rectangular sedimentation tank, yields highly different predictions of solid distribution and removal rate. On the other hand, the main features of the hydrodynamic field are qualitatively similar. Tamayol and Firoozabadi (2006) studied the effects of different turbulent models on the flow field. Tamayol *et al.* (2010) also studied the hydrodynamics of secondary settling tanks while using baffles for increasing their performance. They found that it is required to calculate the concentration profiles in the tank, as well as the velocity profiles. Also their

results showed that both Reynolds and Froude numbers are important in determination of the degree of importance of buoyancy forces in sedimentation tanks. In tanks with low buoyancy forces, the problem is due to short circuiting between the inlet and outlet, while in the tanks which are highly stratified, the problematic phenomenon is bottom density currents.

The design of tanks with high deposition rate and hydraulic efficiency requires complete investigation of the effect of particles on the flow hydrodynamics. In addition, the investigation of the physics of sedimentation and its effects on the hydrodynamics of sedimentation tanks are rare.

In this work, experimental and numerical studies are performed to investigate the effect of particles on hydrodynamics of flow field in secondary sedimentation tanks. In the laboratory, the particle-laden flow in a rectangular sedimentation tank is investigated and also a numerical model is developed using the finite volume method with a k- ϵ turbulent model to consider this problem.

2. EXPERIMENTAL SETUP

The experiments were carried out in a horizontal rectangular settling tank. The channel is 8 m long, 0.2 m wide and 0.6 m deep with a smooth bottom and Plexiglas sidewalls. The slope of the channel bed was set to zero, constantly. The inlet baffle has a rectangular cross section whose height, h_0 , is 11 cm. A sharp-edged weir of the height of 32 cm generates the outlet flow. As a result of the weir, the flow had a height of 34 cm in the channel. A schematic diagram of the tank is shown in Fig. 1.

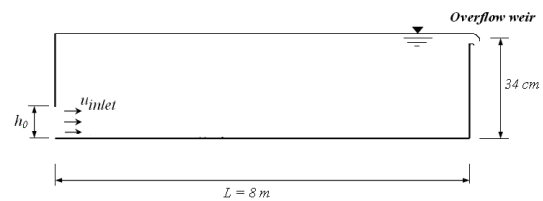


Fig. 1. Schematic sketch of the tank.

A supply tank with a maximum capacity of 2m³ is used to prepare the turbid fluid. The supply tank is made of stainless steel, installed at the elevation of 2.5 m from the ground. A gate valve controls the flow rate to the settling tank, and the flow rate is measured by a flow meter and fixed at a desired rate. This inlet flow rate is 35.5 lit/min in all of the experiments. In this set of experiments, kaolin with the specific gravity of 2.650 was used as the mixture material. After mixing the kaolin within the fresh water in the supply tank and before feeding it into the settling tank, it was transferred to a weir by a circulation pump. The purpose of using this weir was to keep the turbid water head constant and to prevent the impacts of fluctuations in supply tank on the flow rate. In these experiments, the velocity and concentration profiles were measured by a 10 MHz ADV (Acoustic Doppler Velocimeter) made by Nortek Company. Acoustic Doppler anemometry relies on the use of pulsed echo sound wherein an ultrasound pulse is emitted along a measuring probe from a transducer and

the same transducer received the echo reflected from the surface of small particles suspended within the flow, which are assumed to move with the fluid velocity. The scattered sound signal is detected by the receivers and used to compute the Doppler shift. Then, the flow velocity is given from detection of the Doppler shift in the ultrasound frequency as particles pass through the measuring volume.

Concentration is one of the most important physical quantities in sedimentation tanks. In this work, acoustic backscattering technique was used to measure the concentration of particles. This method was previously used by other researchers (Lohrmann *et al.* 1994; Hosseini *et al.* 2006). The measurements began a few minutes after the current had reached the steady state condition, having a constant overflow of 34 cm. The data acquisition took 40–45 seconds for each probe's position. The measurement for each location started from the top of the flow and continued into the lower part by dipping the probes until all the desired positions were selected. About fourteen positions were required to get the velocity profile for each location. By using two probes, velocities were measured simultaneously in two stations with a 1 meter distance along the channel. The station pairs were 1.5, 2.5, 3.5, 4.5, 5.5 m far from the inlet. The total duration of each experiment was about 60 min. A schematic sketch of the experimental setup is shown in Fig. 2.

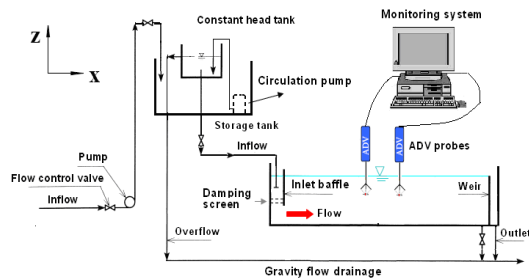


Fig. 2. A schematic sketch of the experimental setup.

To make sure of the consistency of results, each experiment was performed several times. Results show that there is a good degree of repeatability of collected data in a way that the velocity and concentration profiles would fit on each other when an experiment was repeated. In Fig. 3 and Fig. 4 a typical comparison of measured velocity profiles and concentration profiles are shown.

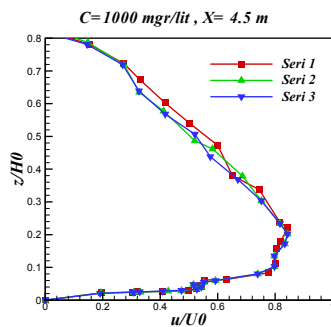


Fig. 3. Typical comparison of three repeats to show the reproducibility of velocity profiles.

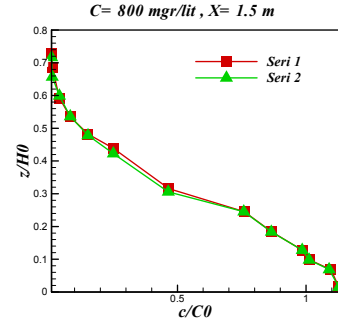


Fig. 4. Typical comparison of two repeats to show the reproducibility of concentration profiles.

3. MATHEMATICAL MODELING

3.1 Governing Equations

Due to low concentration of flow in settling tank, the fluid could be assumed Newtonian. In addition, due to this small concentration, the Boussinesq approximation can be applied; namely the effects of density difference are neglected in the inertial term, but included in the buoyancy force term. Based on these assumptions, the steady state governing equations are as follows:

$$\frac{\partial u}{\partial x} + \frac{\partial v}{\partial y} = 0 \quad (1)$$

$$u \frac{\partial u}{\partial x} + v \frac{\partial u}{\partial y} = -\frac{1}{\rho_w} \left(\frac{\partial p}{\partial x} \right) + \frac{\partial}{\partial x} \left(\mathcal{G} \frac{\partial u}{\partial x} \right) + \frac{\partial}{\partial y} \left(\mathcal{G} \frac{\partial u}{\partial y} \right) + \frac{\partial}{\partial x} \left(\nu_t \frac{\partial u}{\partial x} \right) + \frac{\partial}{\partial y} \left(\nu_t \frac{\partial u}{\partial y} \right) \quad (2)$$

$$u \frac{\partial v}{\partial x} + v \frac{\partial v}{\partial y} = -\frac{1}{\rho_w} \left(\frac{\partial p}{\partial y} \right) + \frac{\partial}{\partial x} \left(\mathcal{G} \frac{\partial v}{\partial x} \right) + \frac{\partial}{\partial y} \left(\mathcal{G} \frac{\partial v}{\partial y} \right) + \frac{\partial}{\partial x} \left(\nu_t \frac{\partial v}{\partial x} \right) + \frac{\partial}{\partial y} \left(\nu_t \frac{\partial v}{\partial y} \right) + g' \quad (3)$$

In which u, v are the velocity components in the flow and vertical directions; p is the pressure, \mathcal{G} is the kinematic viscosity and g' is the reduced gravity and is given by Eq. (4). The density ρ is assumed to be related linearly to the concentration as given by Eq. (5),

$$g' = g \left(\frac{\rho - \rho_w}{\rho_w} \right) \quad (4)$$

$$\rho = \rho_w + c(\rho_p - \rho_w) \quad (5)$$

where g is the gravity acceleration. The equation for conservation of mass is given by Eq. (6) in which c is the concentration of suspended solids and v_s is the particle settling velocity, which is given by the Stokes's equation and given by Eq. (7).

$$\frac{\partial(uc)}{\partial x} + \frac{\partial(vc)}{\partial y} = \frac{\partial}{\partial x} \left(\nu_t \frac{\partial c}{\partial x} \right) + \frac{\partial}{\partial y} \left(\nu_t \frac{\partial c}{\partial y} \right) + \frac{\partial}{\partial y} (\nu_s c) \quad (6)$$

$$v_s = g D_p^2 \left(\frac{\rho_p - \rho_w}{18\mu} \right) \quad (7)$$

ν_t is turbulent viscosity of the flow. The eddy diffusivity is expressed here as a ratio of effective

diffusivity of the solid concentration to the Schmidt number σ_c .

D_p is the particle diameter ($D_p = 11\mu m$), μ is dynamic viscosity, ρ_w is the water density and ρ_p is the particle density ($\rho_p = 2650 kg/m^3$).

3.2 Turbulence Modeling

Turbulence is an intrinsic feature of flows in settling tanks, and provision must be made to incorporate the effects of turbulence in the model. For this purpose, the k- ϵ model is used. In the k- ϵ model, assumptions about the relationship between k and ϵ , and between the eddy viscosity and these two quantities, lead to the set of equations.

$$\rho \frac{dk}{dt} + \rho u_i \frac{\partial k}{\partial x_i} = \frac{\partial}{\partial x_i} \left[\left(\mu + \frac{\mu_t}{\sigma_k} \right) \frac{\partial k}{\partial x_i} \right] + G_k + G_b - \rho \epsilon \quad (8)$$

$$\rho \frac{d\epsilon}{dt} + \rho u_i \frac{\partial \epsilon}{\partial x_i} = \frac{\partial}{\partial x_i} \left[\left(\mu + \frac{\mu_t}{\sigma_\epsilon} \right) \frac{\partial \epsilon}{\partial x_i} \right] + C_{1\epsilon} \frac{\epsilon}{k} G_k + C_{1\epsilon}(1 - C_{3\epsilon}) \frac{\epsilon}{k} G_b - C_{2\epsilon} \rho \frac{\epsilon^2}{k} \quad (9)$$

In which G_k is production of turbulent kinetic energy and G_b is production by buoyancy. Due to small concentration, the Boussinesq approximation can be applied and hence these two terms are given by

$$G_k = \mu_t \left(\frac{\partial u_i}{\partial x_j} + \frac{\partial u_j}{\partial x_i} \right) \frac{\partial u_i}{\partial x_j} \quad (10)$$

$$G_b = - \frac{\mu_t}{\rho S c} \frac{\partial c}{\partial x_i} g_i \quad (11)$$

Turbulent model constants are given by [Kleine and Reddy \(2005\)](#).

$$\sigma_k = 1, \sigma_\epsilon = 1.3, C_{1\epsilon} = 1.44, C_{2\epsilon} = 1.92, C_{3\epsilon} = 0, C_\mu = 0.09$$

Due to small concentration and horizontal bed, the effects of buoyancy production can be neglected ([Firoozabadi et al. 2009](#)).

3.3 Boundary Conditions

The flow is assumed to enter the channel with uniform velocity and concentration. At the outflow boundary the stream wise gradients of all variables are set to zero. It is expected that modeling of the outlet has only a local effect on the flow field.

At the free surface, symmetry condition is applied that includes zero gradients and zero fluxes perpendicular to the boundary except wind shear stress which is imposed by [Eq. \(12\)](#), by horizontal velocity that due to wind effects. At the rigid walls, due to the no slip conditions velocities are set to zero ($u = v = 0$). Concentration gradients are also set zero on the rigid walls. Hence, for the concentration equation, zero gradient conditions normal to the vertical walls are applied. Also for the k- ϵ equations, at the free surface, no flux conditions are

imposed and at the inlet $k_{in} = 0.2u_{in}$ and $\epsilon_{in} = c\mu^{3/4}(k_{in}^{3/2}/\ell_m)$ in which $\ell_m = c\mu(0.5H)$ and $c_\mu = 0.09$ ([Kleine and Reddy 2005](#)).

$$g \frac{\partial u}{\partial n} = \frac{\rho_{air}}{\rho_w} a_{wind} \overline{W} \left\| \overline{W} \right\| \quad (12)$$

In which a_{wind} is wind acceleration which for wind velocity less than 5m/s is 0.000565 ([Hervouet 2007](#)).

3.4 Solution Procedure

The mean flow and the turbulence equations are solved to obtain the velocity and concentration distribution. Orthogonal grids were used, with high resolution near all solid boundaries. The grid independent results are shown in [Fig. 5](#). The final grid which was used is 95×800 .

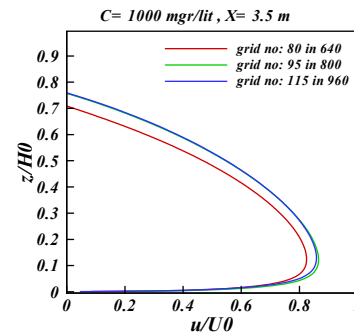


Fig. 5. A typical streamwise velocity with different grid sizes.

3.5 Solver

A finite volume in-house CFD code was developed by using the pressure correction scheme SIMPLEC and a collocated grid arrangement with Rhie-Chow interpolation. The first-order accurate hybrid scheme was first used to discretize the momentum, turbulence, and diffusion equations, but subsequently, the third-order accurate QUICK scheme was applied. These equations were solved with a coupled tridiagonal matrix solver (TDMA). All the fluid properties were treated as constant. The pressure gradient is determined iteratively to satisfy the overall continuity equation; the estimated value is adjusted until the calculated mass flow rate agrees with the specified total inlet mass flow rate. Under-relaxation was introduced in the iterative process with relaxation factors 0.4 for pressure, 0.8 for velocity and k and ϵ . Iteration process was considered converged when the normalized changes between successive iterations decreased to a value of 10^{-4} .

4. VERIFICATION

[Figures 6 and 7](#) compares velocity and concentration profiles with the experimental data in different inlet conditions. They are chosen randomly and all values have errors less than 10% of standard deviation. Standard deviation was calculated as follows

$$\sigma = \left[\frac{1}{n-1} \sum_{i=1}^n (u_i - \bar{u})^2 \right]^{1/2} \quad (13)$$

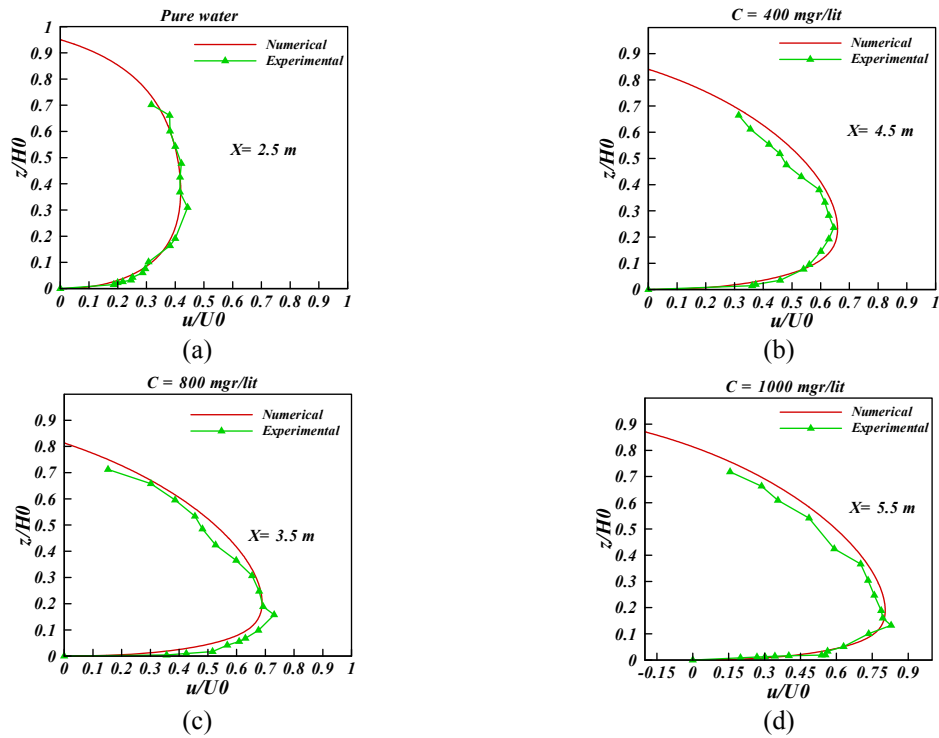


Fig. 6. Comparison of velocity profiles with the experimental data for different inlet concentrations: (a) pure water; (b) $c_{in}=400$ mgr/lit; (c) $c_{in}=800$ mgr/lit; (d) $c_{in}=1000$ mgr/lit.

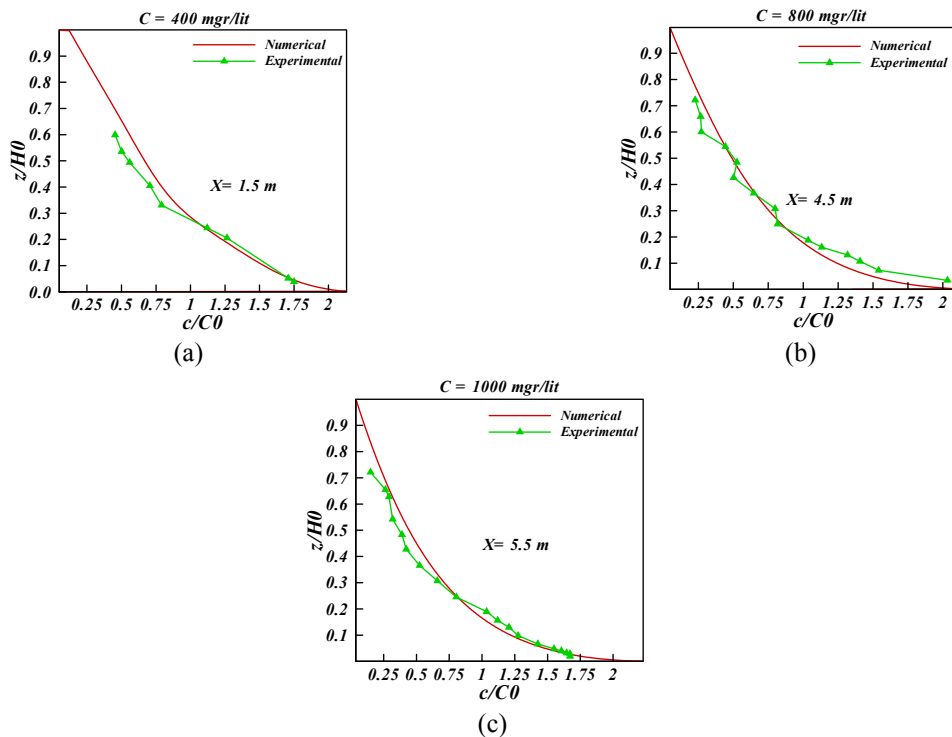


Fig. 7. Comparison of concentration profiles with the experimental data in different inlet concentrations: (a) $c_{in}=400$ mgr/lit; (b) $c_{in}=800$ mgr/lit; (c) $c_{in}=1000$ mgr/lit.

In which u_i is the average velocity in x direction along the channel and \bar{u} is the measured mean velocity in each experiment and was calculated as follows

$$\bar{u} = \frac{1}{n} \sum_{i=1}^n u_i \quad (14)$$

According to Fig. 6, experimental results show that as the concentration increases, a reclining velocity profile

will be generated near the channel bed, so the shear stress in the wall and maximum streamwise velocity are increased. Also negative horizontal velocity shows that surface return flow occurs near the top of the tank.

According to Fig. 7, experimental results show that low concentration occurs in the top of tank and high concentration near the bed. Then in this view, concentration profiles approximately are similar. However, it is noted that x axis is normalized by the inlet concentration. Therefore, the concentration magnitudes at the bed are different for each case shown in Fig. 7.

5. RESULTS AND DISCUSSION

In this work, the effect of particles on flow patterns in the sedimentation tanks was investigated, numerically. There are important parameters which influence the flow structure; for example shear stress at the bottom of the tank, height of the negative streamwise velocity, dead zone, maximum streamwise velocity and its corresponding height from the bottom, and finally the fully develop regions. These parameters can be useful for understanding the structure of sedimentation in settling tanks. Figure 8 shows a schematic diagram of the velocity profiles and its important features.

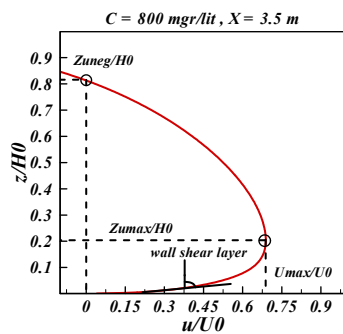


Fig. 8. Schematic diagram showing parameters influenced the flow structure.

Due to high non-steadiness in laboratory conditions, the beginning region was not investigated. In Fig. 9, the effects of concentration on non-dimensional shear stress at the bottom are shown. This was calculated as follows.

$$C_d = \frac{\tau_w}{0.5\rho U_0^2} = \frac{\mu(\partial u \partial y)|_{y=0}}{0.5\rho U_0^2} \quad (15)$$

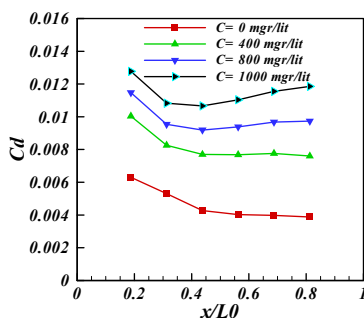


Fig. 9. Shear stress coefficient at the bottom of tank for various inlet concentrations.

In which C_d is the shear stress coefficient at the bottom of the tank and τ_w is the bottom shear stress. According to Fig. 9, C_d in pure water is considerable smaller than that of the particle-laden flows. A higher concentration causes a higher sedimentation. Causing a higher sedimentation, leading to a rise in normal velocity on negative direction so streamwise velocity profile is conducted to near bottom thus rising $C_d \cdot C_d$ decreases at the beginning of the channel then increases along its length. Causing a higher sedimentation along the channel, leading to rise in C_d . It reduces with increasing concentration; hence, C_d is approximately constant in pure water.

Table 1 shows the circulation area at the beginning region in various inlet concentrations. According to Table 1, as c_{in} increases, the magnitude of circulation area decreases. A higher concentration causes a higher stability in the tank, thus reducing the circulation area.

Table 1 Circulation area at the beginning of the channel for various inlet concentrations.

c_{in} (mgr/lit)	Circulation area (m ²)	Circulation area on total area of tank in percent
0	0.245069	9.01
400	0.115557	4.25
800	0.098939	3.64
1000	0.0747	2.75

Figure 10 shows streamlines at the initial region of the channel for various inlet concentrations. Circulation area at the ending region is neglected in comparison with the beginning region. According to Fig. 10, the circulation area obviously decreases as concentration increases. Also a higher concentration causes streamlines getting closer together.

In Fig. 11, effects of inlet concentration on the maximum streamwise velocity are shown. According to Fig.11, as c increases the magnitude of maximum streamwise velocity increases. A higher concentration causes a higher settling; leading to a rise in normal velocity in negative direction, so the streamwise velocity increases. u_{max} decreases at the beginning of the channel then increases along it.

In Fig. 12, effects of inlet concentration on the height of the maximum streamwise velocity from the tank's bed are shown. According to Fig. 12, as c_{in} increases the magnitude of $Z_{u_{max}}$ decreases. A higher concentration causes a higher settling; and a higher sedimentation, leading to a rise in normal velocity in the opposite direction. So the streamwise velocity profile is retained down to near bottom; thus reducing $Z_{u_{max}}$.

In Fig. 13, the effects of concentration on the height of the negative horizontal velocity from the bottom of tank are shown. According to Fig. 13, as c increases the magnitude of Z_{uneg} decreases. This causes a higher

sedimentation, leading to a rise in normal velocity in the opposite direction so horizontal velocity profile is pushed down to near bottom thus reducing Z_{uneg} .

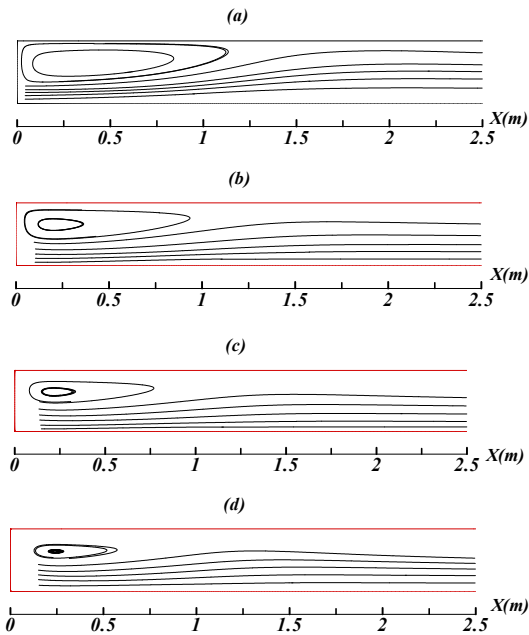


Fig. 10. Streamlines at the beginning of the channel for various inlet concentrations: (a) pure water; (b) $c_{in}=400$ mgr/lit; (c) $c_{in}=800$ mgr/lit; (d) $c_{in}=1000$ mgr/lit.

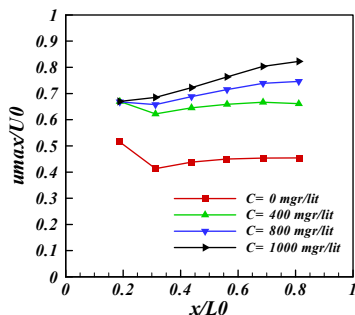


Fig. 11. Maximum streamwise velocity along the channel.

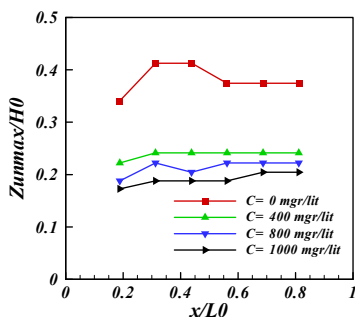


Fig. 12. Height of the maximum streamwise velocity from the tank's bed along the channel.

Figure 14 shows the flow pattern for pure water in the tank. According to Fig. 14, surface return flow occurs in the top of tank because of wind effects. Due to considerable effects of wind on the flow pattern, it cannot be negligible and we considered it based on the empirical relation of Hervouet (2007).

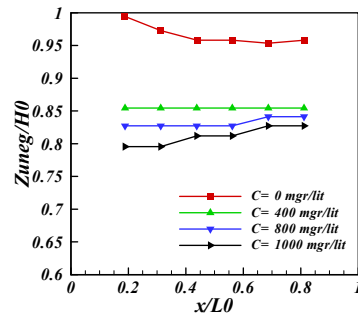


Fig. 13. Height of the negative horizontal velocity from the bottom of tank along the channel.

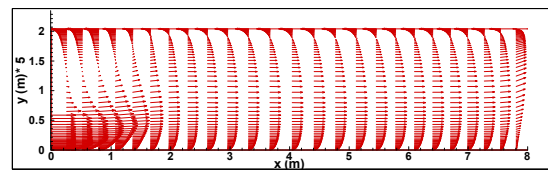


Fig. 14. Flow pattern for pure water in the tank.

In Fig. 15, effects of inlet concentration on the velocity profiles at different sections are shown. According to Figs. 15a and 15b, from $x = 4.5\text{m}$ to $x = 6.5\text{m}$, the velocity profiles are similar showing the fully developed condition. After that, the outflow affects the velocity profile at $x = 7.5\text{m}$. Velocity profiles in Fig. 15d are not similar in any section so there is no fully developed region.

Table 2 Fully developed region for various inlet concentrations from the inlet.

C (mgr/lit)	Fully developed region (m)
0	4.5 – 6.5
400	4.5 – 6.5
800	5.5 – 6.5
1000	–

Table 2 shows the fully developed sections at different inlet concentrations. It is observed that as c_{in} increases the location of the fully developed region moves toward the downstream end of the tank. In case $c_{in}=1000$ mg/lit, there is no fully developed region. For explanation of this phenomenon, the streamwise velocity distributions should be considered. As c_{in} increases particles do significantly settle at further regions along the tank; as a results the maximum velocity increases and its location shifts downwards constantly. On the other hand, in case of $c_{in}=1000$ mg/lit the outflow may affect the velocity profiles. So in this case, no fully developed region was observed.

6. CONCLUSION

A series of laboratory experiments were conducted to study the particle's effect on flow structure in the sedimentation tanks, and the numerical simulation was developed to study the particle-laden flow in the tank. Specific conclusions of this study were:

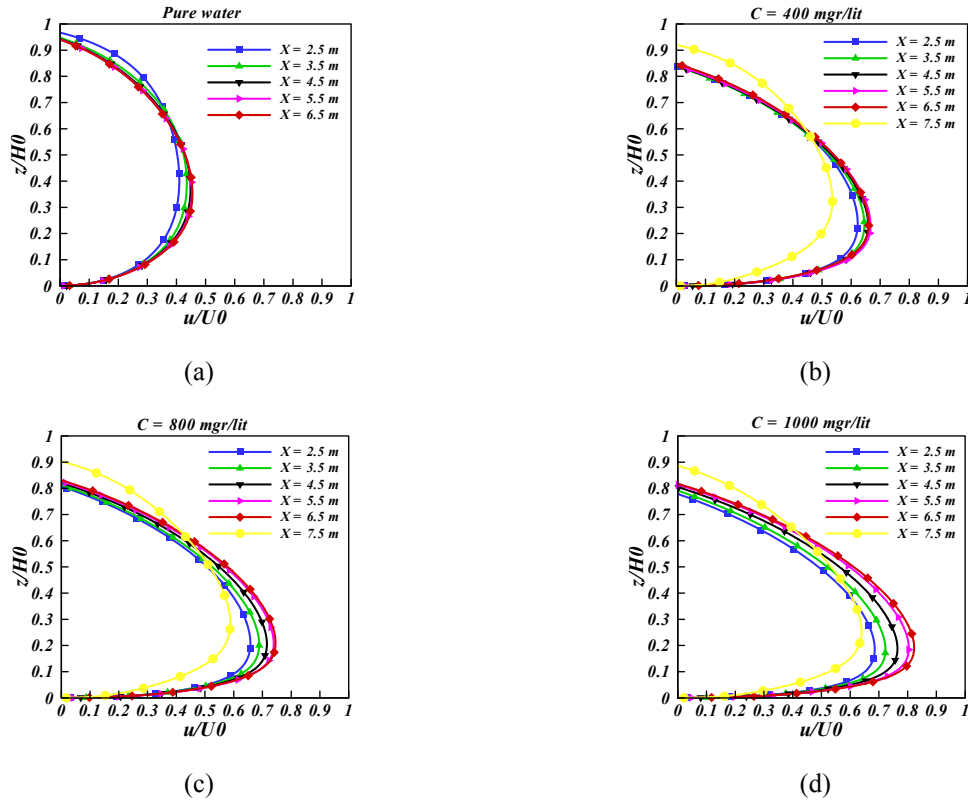


Fig. 15. Effect of inlet concentrations on the velocity profiles at different sections: (a) pure water; (b) $c_{in}=400$ mgr/lit; (c) $c_{in}=800$ mgr/lit; (d) $c_{in}=1000$ mgr/lit.

- Wind has important effects on the flow pattern in sedimentation tank so, it cannot be neglected.
- The results of numerical simulation with k- ϵ model agree well with the experimental data.
- Particles completely change the flow structure. Hydrodynamic parameters are totally different in water-containing particles compared to pure water.
- A higher inlet concentration causes a higher settling; causing a higher sedimentation, leading to a rise in horizontal velocity in opposite direction; so the streamwise velocity profile is pushed down to near bottom thus rising C_d , reducing $Z_{u_{max}}$ and $Z_{u_{neg}}$.
- A higher normal velocity in negative direction because of mass conservation causes a higher streamwise velocity so increases u_{max} .
- As c_{in} increases, the magnitude of circulation area decreases.

As c_{in} increases, the flow becomes fully developed farther from the inlet.

REFERENCES

- Celik, I., and W. Rodi (1985). Prediction of Hydrodynamic Characteristics of Rectangular Settling Tanks. *Int. Symp. On Refined Flow Modeling and Turbulence Measurements* 20(1), 641–665.
- Firoozabadi, B., H. Afshin, E. Aram, (2009). Three Dimensional Modeling of Density Current in Straight Channel. *Journal of Hydraulic Engineering, ASCE* 41(6), 623-630.
- Hervouet, J.M. (2007). *Hydrodynamics of Free Surface Flows: Modeling with the finite element method.* John Wiley & Sons Ltd, England, 13-18.
- Hosseini, S.A, A. Shamsai, B. Ataie-Ashtiani (2006). Synchronous Measurements of the Velocity and Concentration in Low Density Turbidity Currents using an Acoustic Doppler Velocimeter. *Flow Measurement and Instrumentation* 17, 59–68.
- Imam, E. and J.A. McCorquodale (1983). Simulation of Flow in Rectangular Clarifiers. *Journal of Environmental Engineering* 109(30), 713-730.
- Kerbs, P. (1995). Success and Shortcomings of Clarifier Modeling. *Wat. Sci. Tech.* 2(31), 181-191.
- Kleine, D., and B.D. Reddy (2005). Finite Element Analysis of Flows in Secondary Settling Tanks. *Journal for Numerical Methods in Engineering* 64, 849–876.
- Lohrmann, A., R. Cabrera, N.C. Karus (1994). Acoustic Doppler Velocimeter for Laboratory use. *Proc, Symposium on Fundamental and advancements in Hydraulic measurements. ASCE.*, New York, 351-365.
- Mazzolani, G., F. Pirozzi, and G.D. Antoni (1998). A

Generalized Settling Approach in the Numerical Modeling of Sedimentation Tanks. *Wat. Sci. Tech.* 3(38), 95-102.

Stamou, C.R and W. Rodi, (1990). Evaluating the Effect of Geometrical Modification on the Hydraulic Efficiency of Water Tanks Using Flow Through Curves and Mathematical Models. *Journal of Hydro Informatics, ASCE* 20(1), 77-83.

Tamayol, A., B. Firoozabadi, M. A. Ashjari, (2010). Hydrodynamics of Secondary Settling Tanks and Increasing Their Performance Using Baffles. *Journal of Environmental Engineering, ASCE* 136(1), 32-39.

Tamayol, A., B. Firoozabadi, G. Ahmadi, (2008). Effects of Inlet Position and Baffle Configuration on Hydraulic Performance of Primary Settling Tanks. *Journal of Hydraulic Engineering, ASCE* 134(7), 1004-1009.

Tamayol A., and B. Firoozabadi, (2006). Effects of Turbulent Models and Baffle Position on Hydrodynamics of Settling Tanks. *Scientia Iranica* 13(3), 255-260.

Zhou, S., C. Vitasovic, J.A. McCorquodale, S. Lipke, M. DeNicola, and P. Saurer, (1997). Improving Performance of Large Rectangular Secondary Clarifiers. *Proceedings of the 70th Annual WEF Conference and Exposition*, Chicago, USA.